Structural Analysis of Historical Constructions – Jerzy Jasieńko (ed)
© 2012 DWE, Wrocław, Poland, ISSN 0860-2395, ISBN 978-83-7125-216-7

PHYSICAL AND COMPUTATIONAL DISCRETE MODELLING OF MASONRY VAULT COLLAPSE

Tom Van Mele[1], *James McInerney*[2], *Matthew J. DeJong*[3], *Philippe Block*[4]

ABSTRACT

Masonry structures have demonstrated remarkable capacity to withstand large displacements and remain stable. For structures with single curvature (e.g. barrel vaults), which can be readily simplified to two dimensions, stability under large support displacement has been well described using analytical, numerical and physical methods. Structures with double curvature, however, have typically been analysed in two-dimensions in a similar fashion, despite their truly three-dimensional behaviour.
In this paper, the three-dimensional mechanisms formed during large support displacements of a doubly curved masonry groin vault are investigated using physical and computational models. The study focuses on three aspects: 1) evaluation of three-dimensional mechanisms, 2) determination of the displacement magnitudes that lead to collapse, and 3) evaluation of the ability of computational methods to predict the experimental results.
The collapse of a 3D-printed groin vault scale model under actuator-controlled support displacements was captured with an optical measuring system, and the measured displacement capacities were compared with Discrete Element Modelling results.
The physical and computational results both predict the expected large displacement capacity, and the sensitivity of the discrete element results to a variety of parameters is quantified. In addition, a more complete understanding of the stability of masonry vaults is obtained, particularly of the relation between support movements and three-dimensional collapse mechanisms. More generally, the research methodology introduces new, promising improvements in the analysis of complex masonry structures.

Keywords: *Masonry, Vaults, Collapse, Discrete Element Modelling, 3D-printing, Scale model testing, Stability*

1. INTRODUCTION

1.1. Equilibrium analysis

Unlike modern structures, stability and not stress is of primary concern for many historic masonry structures [1, 2]. Because masonry often has no, or very little, capacity to resist tension, it has to be shaped such that it acts in compression only. To apply equilibrium analysis for the assessment of the stability and safety of masonry structures, Heyman [3] formalized the limit analysis framework, based on three key assumptions: masonry has no tensile capacity, sliding does not occur at voussoir interfaces, and the masonry itself is considered rigid. These assumptions have been widely used to successfully predict two-dimensional stability of complex vaulted structures.

1.2. Physical and computational methods for discrete modelling of masonry

1.2.1. Physical (scale) modelling

If the stability of masonry structures is mainly a question of geometry and not of material failure, the behaviour of these structures can be considered independent of scale, and can thus be investigated and understood using scale models [3, 4]. Ancient builders allegedly used this scale independency in

[1] Postdoctoral Researcher, Inst. of Technology in Architecture, ETH Zurich, Switzerland, vanmelet@ethz.ch
[2] Doctoral Researcher, University of Cambridge, Cambridge, UK, jbm46@cam.ac.uk
[3] PhD, Lecturer, University of Cambridge, Cambridge, UK, mjd97@cam.ac.uk
[4] PhD, Assistant Professor, Inst. of Technology in Architecture, ETH Zurich, Switzerland, pblock@ethz.ch

different ways: small scale models were used to investigate and understand the stability of new structural designs and geometries, whereas scaled versions of tried-and-tested designs were often reused in new projects. Similarly, drawings by Danyzy [5] indicate the use of arch and buttress plaster models to investigate collapse mechanisms due to support displacements.
More recently, physical scale models have been used to investigate the collapse behaviour of two-dimensional masonry structures subjected to differential support displacements [6, 7], or seismic loading [8]. However, studies of the equilibrium of three-dimensional masonry structures using scale models are less common. The first detailed assessment using 3D-printed scale models addressed the equilibrium of cracked masonry domes [9, 10].

1.2.2. Computational modelling

Discrete element modelling (DEM) has emerged as an important computational method in understanding the behaviour of masonry structures, as it has the capacity to treat masonry blocks as separate units. Unlike continuum analysis techniques, DEM considers systems of separate interacting bodies and is designed to deal with contact and stability.
DEM methods fall into two primary categories, those with 'compliant contacts' and those with 'unilateral contacts'. Compliant contact formulations use contact springs to determine contact forces, while unilateral contact methods use non-smooth contact formulations which do not allow any penetration between adjacent blocks. Both methods have been used to model masonry structures. In particular, numerous researchers have used two-dimensional compliant contact methods for the investigation of arch bridges (e.g. [11]), retaining walls (e.g. [12]), and the response of various structures to seismic loading [13, 14]. Fewer studies consider three-dimensional stability, although Lemos [15] investigated the 3D stability of intersecting masonry arches under static and dynamic loading. Critically, relatively few studies which use DEM to investigate large displacements and collapse have compared modelling predictions with experimental results.

1.3. Objectives

While two-dimensional stability is well-understood, there is a need for more robust and more accurate methods for 3D equilibrium analysis of masonry structures (and rigid block assemblies in general) especially for large displacement analyses. In this paper, the capacity of masonry cross-vaults to withstand differential support displacements will be investigated using both physical and computational models, using a generic groin vault geometry. The aim is to quantify the displacement capacity, and more importantly to compare the modelling methods and evaluate the validity of both approaches, including the assumptions, advantages, limitations and challenges. This research is part of a larger research project that aims to develop better understanding in the three-dimensional (collapse) behaviour of masonry structures, and to improve physical and computational methods for analysis of existing masonry structures.

2. METHODOLOGY

2.1. Physical modelling

The physical model experiments were conducted in a custom-made testing laboratory developed by the BLOCK Research Group at ETH Zurich [16]. The facility has the capability to accurately measure the displacement and collapse behaviour of 3D-printed scale models under applied loads and differential support movements. The set-up consists of two main components: an actuated testing table and a high-speed, non-contact, optical measuring system, as seen in Figure 1.
The surface of the testing table is divided into 28 segments that can be displaced independently and continuously by horizontal and vertical linear actuators (FESTO [17]) with ±0.05 mm and ±0.07 mm accuracy, respectively, at a speed of 0.1 up to 30 mm/s. The ball-jointed base with two large actuators also allows for global tilt tests to simulate combined horizontal and vertical loading. The optical measuring system is the PONTOS dynamic 3D motion analysis system by GOM [18].
The individual blocks of scale (vault) models are printed with a ZPrinter 650 by 3D Systems [19]. This high-resolution, colour 3D-printer with an accuracy of 0.1 mm allows printing the dotted targets required by the measuring system directly onto and together with the blocks (Fig. 1). Each block is labelled with minimum three dots forming a unique pattern among all the blocks in the model. These patterns are recognized by the analysis software as a representation of a rigid body of which the movement can be traced and reconstructed.

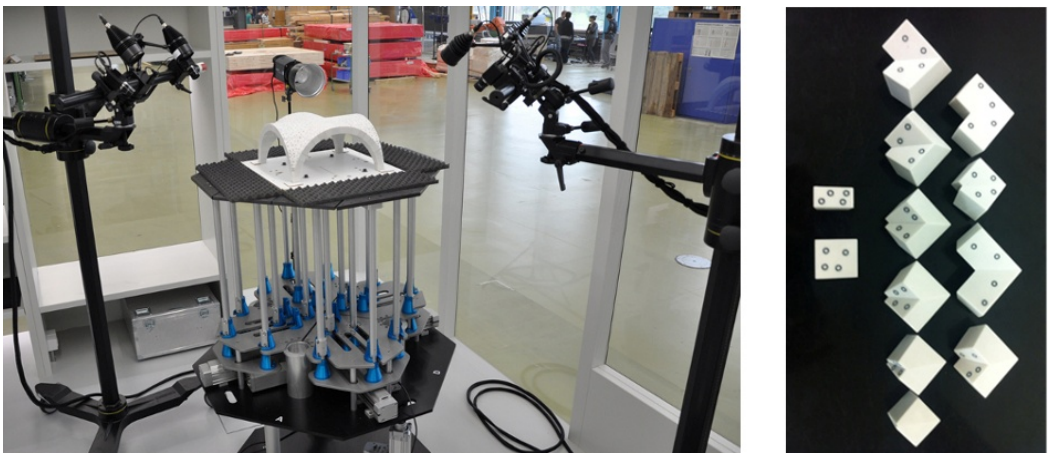

Fig. 1 Actuated testing table and measuring equipment in the BLOCKlab at ETH Zurich (left), and a collection of 3D-printed pieces with unique dot pattern (right)

2.2. Computational modelling

The response of the cross-vault to displacement loading was simulated computationally using the three-dimensional DEM software 3DEC [20], which is based on the compliant contact formulation of Cundall [21]. In this modelling framework, contact is controlled by normal and shear joint stiffness, the blocks can be either rigid or deformable, and an explicit solution procedure is adopted for both static and dynamic analyses.

For the cross-vault modelling, rigid blocks were used with a specified material density, friction angle, and normal and shear joint stiffness. The explicit solution procedure uses a time-stepping procedure which requires specification of quasi-static modelling, in which the model is over-damped, or dynamic modelling, which enables dynamic simulation. While 'dynamic' modelling was used for the primary results, the effect of 'quasi-static' versus 'dynamic' modelling was also investigated (see Section 3.2).

2.3. Model geometry

The cross-vault geometry, used for both experimental testing and computational simulation, was generated by two intersecting semi-circular barrels with inner radius of 150mm, as shown in Figure 2. The thickness of the vault is approximately 24.4 mm. The symmetric geometry results in relatively few unique blocks. The vault consists of two types of regular blocks (i.e. a full block and a half block) and 10 different types of groin blocks (see Fig. 1). In total, there are 32 half blocks, 112 full blocks and 40 groin blocks. Thin support blocks were fixed to the base to prevent sliding between the base and the vault. These support blocks were not initially included in the DEM simulations, but their effect was later investigated and is discussed in Section 3.2.

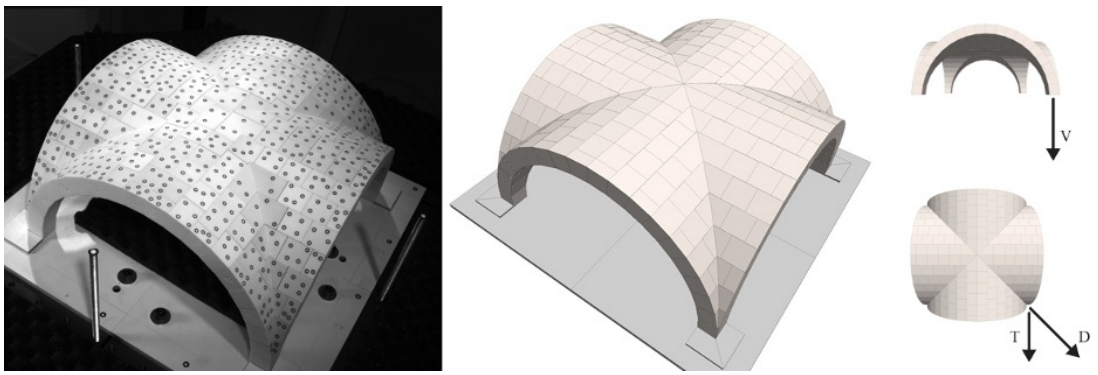

Fig. 2 3D-printed scale model (left) and DEM model (middle) of the cross vault, and the three displacement directions which were investigated (right): transverse (T), diagonal (D), and vertical (V) movement of one of the supports

A digital model of this structure was constructed in Rhinoceros [22] which then served as a basis for the physical and numerical models. For the physical model, custom scripts were written to generate and place unique dot patterns and identification labels on all blocks, produce an optimized stacking for printing, and generate the machine code for fabricating the formwork automatically.

2.4. Material properties and loading

The individual blocks of the physical model were 3D-printed using a composite of zp150 powder and zb61 clear binder [19]. After printing, the blocks were impregnated with Z-Bond 101 [19] for improved strength and durability during the tests. The density and friction angle of these blocks were determined for 10 random samples. The density was measured to be 0.598 ±0.0297 g/cm^3 and the friction angle 43 ±3.464°. The standard deviation on both the measured densities and friction angles can be explained by the fact that there was no possibility to control the amount of hardening fluid that got absorbed by any one block during the impregnation process.

Initially, the experimentally determined average friction angle and material density were used as input for the DEM simulations, along with normal and shear joint stiffness of 100G Pa/m and 70 GPa/m, respectively. The specified joint stiffness is relatively large, allowing negligible inter-penetration between adjacent blocks. Sensitivity of the response to these parameters is discussed in Section 3.2.

Three different displacement directions were investigated: transverse (T), diagonal (D), and vertical (V) movement of one of the supports (Fig. 2). In both the computational and physical experiments, the displacements were applied at low velocities and in small increments to replicate, as closely as possible, the quasi-static support settlement process and allow the models to re-establish static equilibrium between each increment.

3. RESULTS

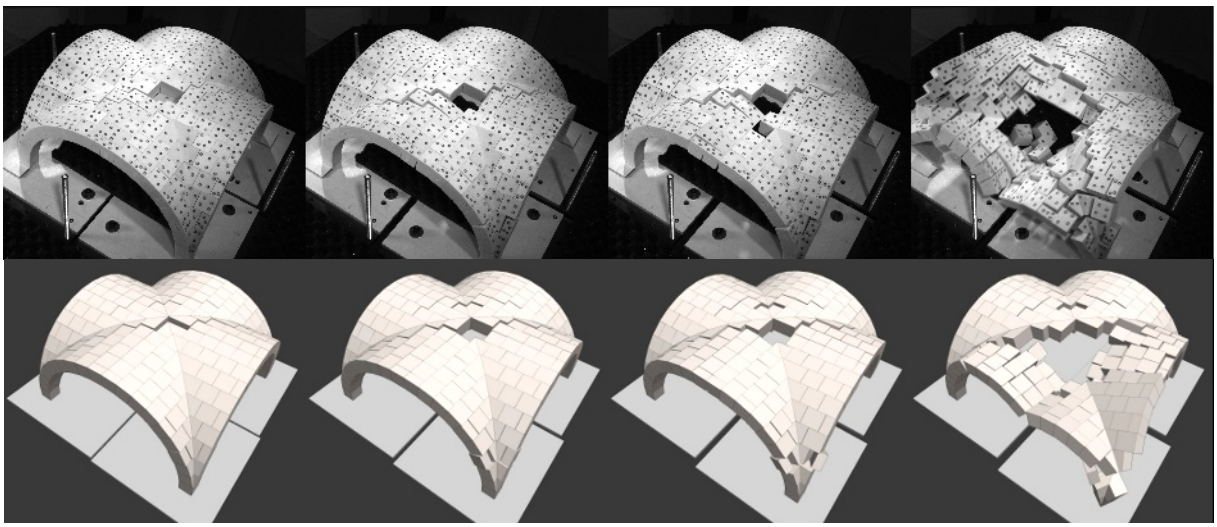

Fig. 3 Collapse mechanisms caused by diagonal displacement of the support. Physical model (top) at 10 mm, 15 mm, 20 mm and 24 mm. Computational model (bottom) at 6 mm, 12 mm, 18 mm and 23 mm

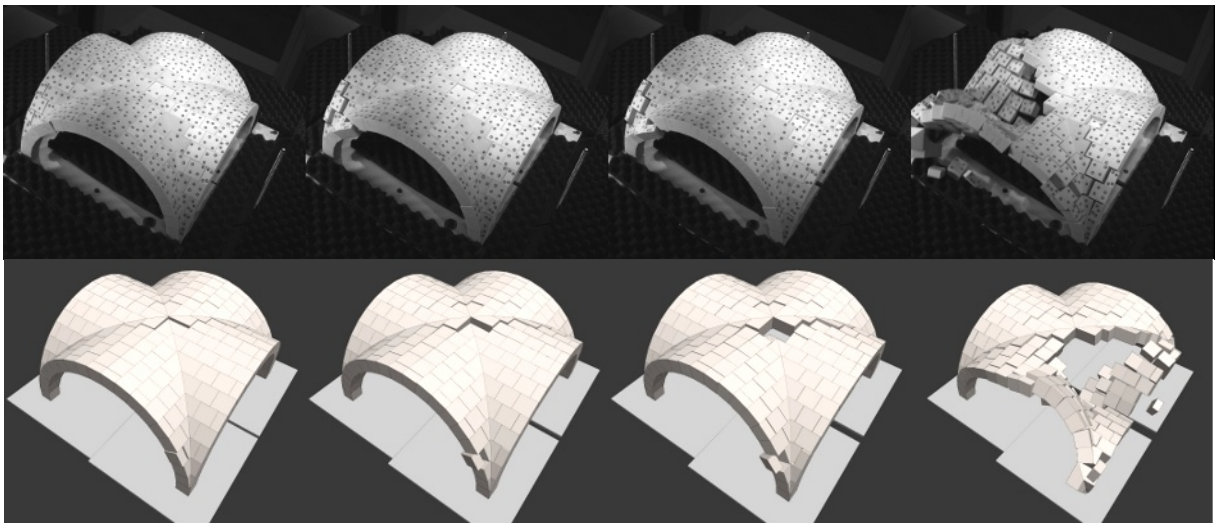

Fig. 4 Collapse mechanisms caused by transverse displacement of the support. Physical model (top) at 5mm, 10 mm, 11 mm, and 12 mm. Computational model (bottom) at 6 mm, 12 mm, 18 mm, and 23 mm

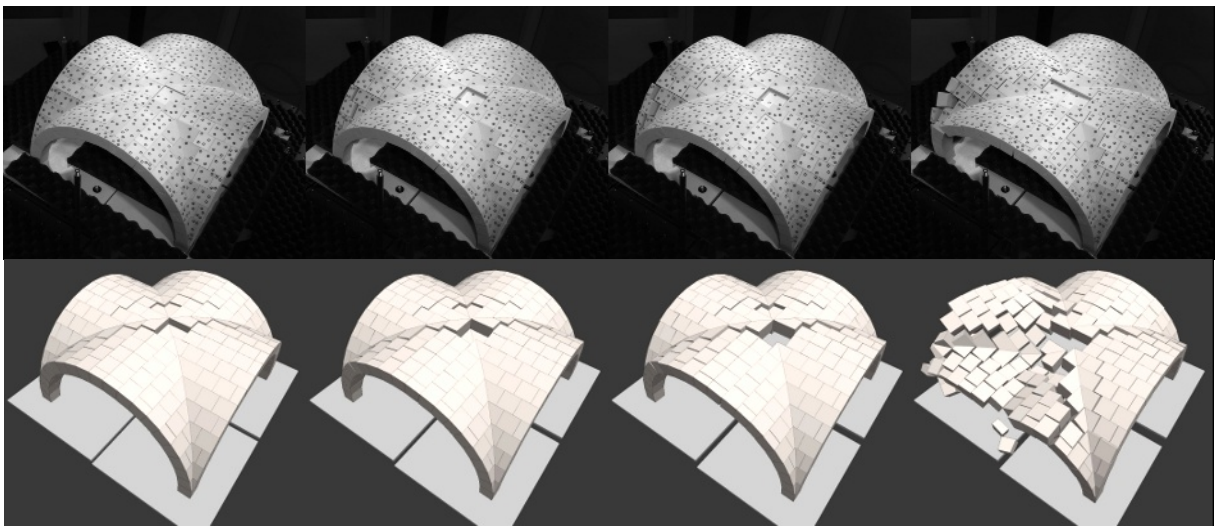

Fig. 5 Collapse mechanisms caused by vertical displacement of the support. Physical model (top): 5 mm, 10 mm, 12 mm, and 13 mm. Computational model (bottom): 12 mm, 18 mm, 24 mm, and 29 mm

The results of the physical experiments and computational simulations are summarized in Table 1, where the applied displacements are recorded both when the first block fell and when the entire vault collapsed. The physical simulations were repeated three times per displacement direction. Figures 3 to 5 give a visual comparison of several stages of the displacement until collapse for the different displacement directions. In all images the displaced support is closest to the camera position.

Table 1 Experimental and computational modelling results

Displacement direction	**1st block fall [mm]**				**Collapse [mm]**			
	physical			**3DEC**	**physical**			**3DEC**
diagonal	10.75	10.23	12.01	11	23.41	24.97	23.79	23
transverse	-	-	-	19	12.23	10.0	12.45	23
vertical	-	-	-	20	14.49	11.8	12.56	29

3.1. Observations

The displacement values and the formed mechanisms at collapse of the physical model are consistent for the different tests in each displacement direction. They result in an average collapse displacement of 24 mm in the diagonal, 12 mm in the transverse, and 13 mm in the vertical direction. In the diagonal case, this compares remarkably well to the computational simulation, which predicted collapse at 23 mm. Also the formed mechanism, i.e. crack pattern and location, is almost identical, as seen in Figure 6.

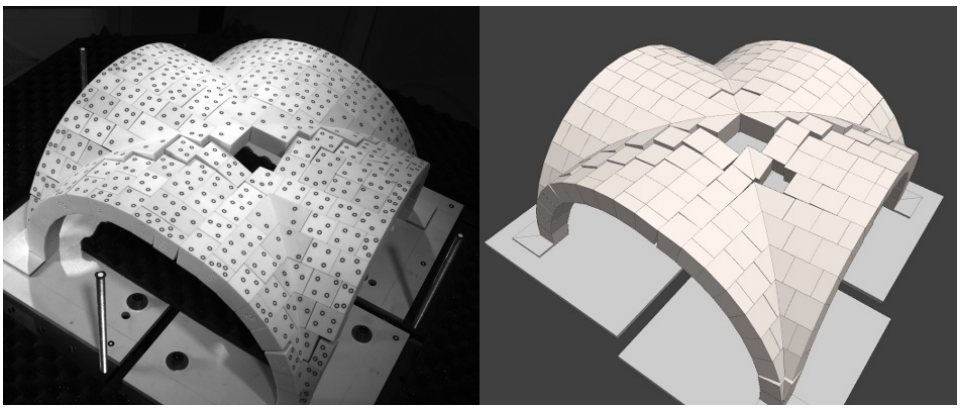

Fig. 6 In the case of diagonal displacement, the collapse behaviour of the physical (left) and computational model (right) is remarkably similar. The hinge locations and crack patterns are almost identical

However, for the transverse and vertical displacement directions, computational simulations predict displacement capacities of 23 mm and 29 mm, respectively, which are significantly higher than the physical modelling results. In the transverse case, the formed mechanism is also different. In the physical model it is clearly the instability of the left support that causes the collapse, whereas in the computational model it is the instability of the displaced support itself. Furthermore, the crack pattern in the computational model clearly runs from the left to the right support, whereas in the physical model it follows the diagonal from the displaced support to the support on the opposite side. The 'premature' collapse of the physical models seems to be caused by the rotational instability of some of the edge blocks. This instability occurs much later (i.e. at much higher displacements) or not at all in the computational models.

Table 2 Results of DEM sensitivity study

Friction Angle f [degrees]	Normal joint stiffness [GPa/m]	Shear joint stiffness [GPa/m]	Analysis	Base support blocks	1st block fall [mm]	Collapse [mm]
43	100	70	dynamic	no	20	29
30	100	70	dynamic	no	25	25
43	10	7	dynamic	no	21	29
43	100	70	quasi-static	no	20	32
43	100	70	quasi-static	yes	23	41

3.2. Sensitivity study

The sensitivity of the DEM results to various modelling parameters was also investigated. Results are shown in Table 2 for applied displacement in the vertical direction. The first row of Table 2 shows the baseline results from Table 1.

Using limit analysis [6], friction is considered sufficient to prevent sliding. While this is a reasonable assumption in two-dimensions, sliding is involved in the formation of mechanisms for doubly curved vaults. The effect of reduced friction was investigated, and caused a slight decrease in the collapse displacement (29 mm to 25 mm), but a slight increase in the displacement at which the first block fell (20 mm to 25 mm). The reason for this is depicted in Figure 7. For the reduced friction case, sliding occurs just above the left (and right) supports. This enables the vault to expand (in plan) while one support moves downward, which better maintains the thrust through the blocks near the vault apex. However, this also reduces the displacement capacity at total collapse.

Although a challenge in DEM is accurately defining the joint stiffness, this difficulty is somewhat alleviated when simulating scale model tests, where contact forces are low. The effect of joint stiffness on the response is shown to have negligible effect for a reduction in stiffness of one order of magnitude. Continued reduction in stiffness would only have an effect when block inter-penetration becomes significant.

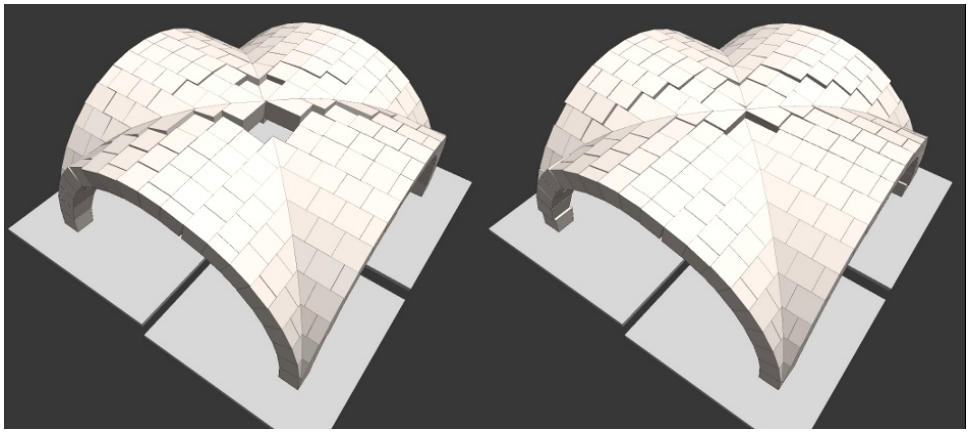

Fig. 7 Comparison of DEM results at 24 mm of vertical displacement: friction angle = 43 (left), 30 (right)

Dynamic simulations were used to achieve the baseline prediction values above, but quasi-static simulations were also conducted and caused an increase in the displacement capacity. This was expected, as the over-damped quasi-static simulations remain standing in remarkably precarious states.

For example, the vault in Figure 8 is in equilibrium, although it would not stand in that state in reality. The smallest imperfection or vibration would cause failure.

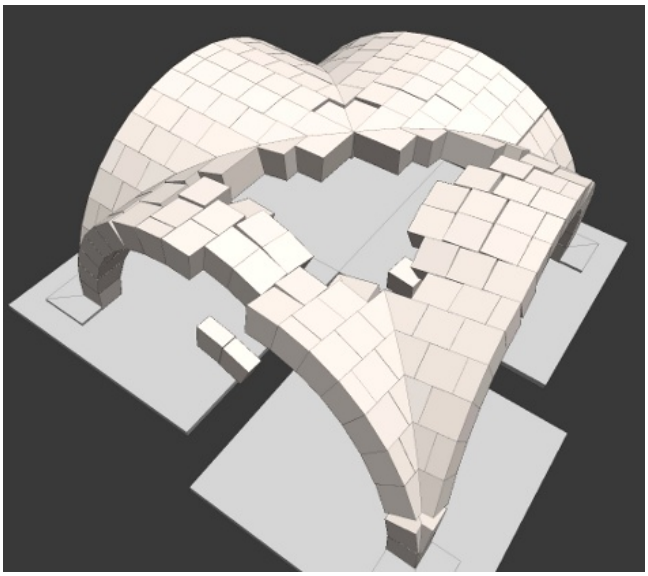

Fig. 8 Unrealistic, heavily displaced state obtained with perfect geometry and quasi-static simulation in DEM

Finally, the effects of the base support which prevent sliding were investigated. Adding support base blocks caused a remarkable increase in the displacement capacity, and the reason for this seems to be largely computational. Due to the large thrust at the base, the friction at these base blocks is also large, and thus sliding is prevented. Due to the perfect geometry, the bottom block of the vault is unrealistically 'locked' in place.

4. DISCUSSION

While the experimental and computational results compare reasonably well, computational results generally over-predicted the displacement capacity. The primary reason for this discrepancy is that the computational model is a 'perfect' assembly of 'perfect' blocks and contact surfaces. As a result, the interlocking between blocks in the computational assembly will be perfect; none of the blocks will be initially loose. While the 3D printed model was remarkably accurate, the assembly, which was done manually, was not perfect. Even slight dislocations can cause very minor hinges and offsets between blocks, which affect the initial geometry and could slightly reduce the effective thickness.

While these reasons account for general differences between the methods, there was particular discrepancy between the displacement values predicted for the transverse and vertical directions. The reason for this is less obvious. For diagonal displacement, the formed mechanism allows the vault joints to open up with less sliding; the vault basically spreads similar to an arch on spreading supports. However, the vertical and transverse displacements force the vault joints to shear and twist. This is evident in the computational collapse mechanism in Figure 4, where the section of vault on the front is twisting and hinging, and in Figure 7, where the vault is shown to spread in plan under vertical displacements when the friction is reduced. Therefore, it seems that this 'shearing' of the vault may have caused the local instability at the left corner of the physical model (Figs. 4 and 5). This might have been due to an extremely slight initial local imperfection at this point, or to a concentration of displacements. Regardless, the perfect geometry in the computational model seems to have prevented this localized failure.

It thus seems that the perfect conditions of the computational simulations generally result in an overprediction of the displacement capacity of the physical scale models. Note, however, that the reduced displacement capacity of the physical models as a result of assembly inaccuracies is most likely magnified due to the scale in comparison to full scale structures. In large structures stresses tend to be higher and therefore contacts more distributed. Additionally, mortar tends to distribute contact pressures even further. On the other hand, in large structures stress concentrations will cause local material failure (i.e. 'crushing'). As a result, point contacts become area contacts and this in turn could reduce the displacement capacity.

5. CONCLUSIONS

This study has used both physical and computational modelling to confirm the relatively large displacement capacity of masonry vaults, and to provide new insights regarding three-dimensional collapse behaviour. The validation of DEM simulations is critical and often overlooked, and physical modelling is vital to determine the confidence that can be placed in computational modelling results.
The results show that initial slight imperfections in scale models may play a different role in the outcome of collapse simulations depending on the direction of support displacements. For spreading problems, imperfections seem to have less effect. In fact, in the case of diagonal displacement, the computational and physical results were almost identical. On the other hand, in cases with more shearing of the vault (i.e. the transverse and vertical displacement direction cases) the effect of initial imperfections seems to be larger. These observed discrepancies demonstrate that, at present, the results of analyses with either approach should be interpreted with care.
Further research should focus on how to deal with imperfections and incorporate them into the modelling process. A possible approach might be to change the testing procedure such that both simulations start with equally imperfect models; for example, by running the computational simulations on the measured geometry of the assembled physical model rather than the perfect geometry of the CAD model.

ACKNOWLEDGEMENTS

The authors would like to thank Ramon Weber and Matthias Rippmann for preparing the Rhino model of the cross vault from the 3DEC models, and Marcel Aubert for constructing the physical model and assisting with the physical experiments.

REFERENCES

[1] Heyman J. (1995) *The Stone Skeleton: Structural engineering of masonry architecture*. Cambridge, Cambridge University Press.
[2] Ochsendorf J. (2002) *Collapse of Masonry Structures*. PhD Dissertation, University of Cambridge, Cambridge, UK.
[3] Heyman J. (1966) The Stone Skeleton. *Int. J. Solids Structures* 2(): 249-279.
[4] Huerta S. (2004) *Arcos bóvedas y cúpulas. Geometría y equilibrio en el cálculo tradicional de estructuras de fábrica*. Madrid, Spain.
[5] Danyzy A.A.H. (1732) Méthode générale pour déterminer la résistance qu'il faut opposer à la poussée des voûtes. *Histoire de la Société des Sciences établie à Montpellier* 2: 40-56.
[6] Ochsendorf J. (2006) The Masonry Arch on Spreading Supports. *The Structural Engineer* 84(2): 29-36.
[7] Romano A., Ochsendorf J. (2006) Masonry circular, pointed and basket handle arches: a comparison of the structural behaviour. In: P.B. Lourenco, P. Roca, C. Modena, S. Agrawal (eds.) *Structural Analysis of Historical Constructions*. New Delhi, India.
[8] DeJong M.J., De Lorenzis L., Adams S., Ochsendorf J. (2008). Rocking stability of masonry arches in seismic regions. *Earthquake Spectra* 24(4): 847-865.
[9] Quinonez A., Zessin J., Ochsendorf J. (2010) Small-Scale Models for the Analysis of Masonry Structures. In: *Proc. of the 7th International Conference on Structural Analysis of Historical Constructions*. Shanghai, China.
[10] Zessin J., Lau W., Ochsendorf J. (2010) Equilibrium of cracked masonry domes. *ICE Engineering and Computational Mechanics* 163: 135-145.
[11] Bicanic N., Stirling C., Pearce C.J. (2003). Discontinuous modelling of masonry bridges. *Computational Mechanics* 31: 60-68.
[12] Powrie W., Harkness R. M., Zhang X., Bush D. I. (2002). Deformation and failure modes of drystone retaining walls. *Geotechnique* 52(6): 435-446.
[13] Azevedo J., Sincraian G., Lemos J.V. (2000) Seismic behavior of blocky masonry structures. *Earthquake Spectra* 16(2): 337-65.
[14] De Lorenzis L., DeJong M.J., Ochsendorf J. (2007) Failure of masonry arches under impulse base motion. *Earthquake Eng Struct Dynam* 36(14): 2119-36.

[15] Lemos J.V. (1998). Discrete element modeling of the seismic behaviour of stone masonry arches. In: G. N. Pande, J. Middleton, B. Kralj (eds.) *Proc. of the Fourth International Symposium on Computer Methods in Structural Masonry*. London.
[16] Block P., Van Mele T., Aubert M. (last visit: 04.05.2012) BLOCK Lab: Structural Testing of Discrete Structures using Rapid Prototyping. http://block.arch.ethz.ch/projects/20.
[17] FESTO (last visit: 04.05.2012) http://www.festo.com.
[18] gom Optical Measuring Techniques (last visit: 04.05.2012) http://www.gom.com.
[19] 3D Systems (last visit: 04.05.2012) http://www.zcorp.com.
[20] 3DEC (last visit: 04.05.2012) http://www.itascacg.com/3dec.
[21] Cundall P.A., Strack O.D.L. (1979). A discrete numerical model for granular assemblies. *Geotechnique* 29: 47-65.
[22] Rhinoceros NURBS modelling for Windows (last visit: 04.05.2012) http://www.rhino3d.com.